International Journal of Modern Manufacturing Technologies
ISSN 2067–3604, Vol. XVI, No. 3 / 2024
https://doi.org/ 10.54684/ijmmt.2024.16.3.143

OPTIMIZATION OF FDM 3D PRINTING PARAMETERS FOR TENSILE STRENGTH OF PETG CARBON FIBRE USING TAGUCHI METHOD

Nor Aiman Sukindar[1], Nurul Aini Athirah Abdul Rahim[2], Ahmad Shah Hizam Md Yasir[3], Shafie Kamaruddin[2], Mohamad Talhah Al Hafiz Mohd Khata[2], Nor Farah Huda Abd Halim[2], Mohamad Nor Hafiz Jamil[2], Ahmad Azlan Ab Aziz[4]

[1]Universiti Teknologi Brunei, School of Design
Tunku Highway, Gadong BE 1410, Brunei Darussalam
[2]International Islamic University Malaysia, Manufacturing and Materials Department
Gombak, Selangor, Malaysia
[3]Rabdan Academy, Faculty of Resilience
65, Al Inshirah, Al Sa'adah, Abu Dhabi, 22041, PO Box: 114646, Abu Dhabi, UAE
[4] Engineering Faculty, Universiti Teknologi Brunei, Jalan Tungku Link Gadong BE1410, Brunei Darussalam

Corresponding author: Nor Aiman Sukindar, noraimansukindar@gmail.com

Abstract: Fused Deposition Modeling (FDM) has become one of the most prevalent technologies in the field of additive manufacturing (AM). Nonetheless, polyethylene terephthalate glycol (PETG), a polymer renowned for its mechanical strength, has been significantly employed in 3D printing as an alternative to traditional materials. The incorporation of fibers renders PETG-based composites viable for a diverse range of applications. However, the tensile strength of PETG carbon fibre developed using FDM depends on multiple printing conditions. Therefore, this work aims to examine the impact of printing parameters (layer thickness, infill density, and printing speed) at three individual levels on the tensile and structural characteristics of PETG carbon fibre. A total of nine print runs were executed by manipulating the three parameters. Three samples were produced for each run to ensure consistency in the results. Tensile tests on the samples were carried out, and a scanning electron microscope (SEM) was used to examine the structure of the printed parts. Finally, L9 (3^3) orthogonal arrays were developed for the experiment. Following that, an analysis of variance (ANOVA) was conducted to determine the crucial factors and their ideal levels. The results showed that the infill density parameter significantly influenced the optimization of the tensile strength of PETG carbon fibre. The optimal value for this parameter was found to be 80%. Increasing the density of the infill improves the tensile strength by reducing the air gaps and decreasing deformation, leading to a solid and tightly packed structure. Thereafter, the most effective settings were identified as a layer thickness of 0.4 mm, an infill density of 80%, and a printing speed of 30 mm/s.
Keywords: FDM 3D printing, PETG carbon fibre, printing parameters, tensile properties, ANOVA

1. INTRODUCTION

Three-dimensional (3D) printing is an additive manufacturing process that generates a three-dimensional solid object from a computer-aided design (CAD) model or digital 3D file. Some of the commonly used filament materials are acrylonitrile butadiene styrene (ABS), polylactic acid (PLA), polyethylene terephthalate glycol (PETG), and nylon. As 3D printing gained popularity, advancements in technology and materials expanded its capabilities, which enabled 3D printing to offer numerous benefits, including the capability to construct complex structural models compared to traditional manufacturing technologies, low startup cost, enhanced production speed, a reduction in waste, and the downsizing of warehouses [1]. 3D printing technology consists of several methods; however, the most widely used process in the industry is FDM. In FDM, complicated geometries are formed by numerically controlled nozzles using layer-by-layer fabrication without clamps, jigs, and fixtures, as in conventional manufacturing processes [2].
Several studies have examined the impact of various printing conditions on the tensile strength of PETG carbon fiber [3-5]. Several process variables, including printing velocity, layer thickness, raster orientation, and infill percentage, significantly impact the quality and printing time of products created through FDM [6]. However, since most of the prior research studied each parameter separately, it is necessary for these essential printing parameters to have a full optimization analysis.

Carbon fiber-reinforced filaments have been extensively studied for their enhanced mechanical properties when combined with various thermoplastic matrices such as PETG, PLA, and polyamide. Research has shown significant improvements in tensile and flexural properties through the optimization of process parameters [7]. Other studies have highlighted the need for careful parameter optimization to achieve the best mechanical properties in carbon fiber-PLA composites [8]. Optimizing parameter selection has also been shown to yield optimal tensile strength in carbon fiber-PETG composites [9], while the incorporation of woven carbon fiber layers into PLA laminates through FDM has achieved significant improvements in both tensile and flexural properties [10].Various printing parameters have a critical impact on the tensile strength of 3D-printed composites. The Taguchi method has been used to assess the impact of infill density, printing speed, and layer thickness on PLA parts, finding that these parameters substantially influence tensile strength [11]. Further studies have aimed to maximize tensile strength in ABS and carbon fiber-PLA materials by optimizing these process parameters [12].

Infill density is a pivotal factor in the mechanical properties of 3D-printed parts, with higher densities generally providing greater strength. Increased infill density has been shown to significantly enhance tensile strength in carbon fiber-PLA composites [8]. An 80% infill density has been found to produce optimal strength and hardness in carbon fiber-PLA parts [9]. Infill density has also been identified as a major factor in improving tensile strength in PLA parts, with optimized settings leading to better mechanical properties [13].Layer thickness and printing speed are crucial for optimizing tensile strength. Reducing layer height has been found to significantly improve tensile properties in carbon fiber-PLA specimens [9]. Optimal tensile performance in PLA parts has been achieved by combining lower layer thickness with moderate printing speed [11]. Additionally, different composites require careful balancing of printing speed; PETG-based materials, for instance, achieve superior bending properties at slower speeds [14].

This study employed the Taguchi technique to examine the impact of printing settings on the tensile strength and microstructure of PETG carbon fibre. The study investigates three printing parameters: layer thickness (mm), infill density (%), and printing speed (mm/s). The assessment of these parameters will determine the ideal parameters that have the primary impact on the mechanical characteristics of PETG Carbon Fibre.

2. MATERIALS AND METHODS

2.1 Sample Fabrication

The samples were created using SolidWorks Software (Dassault Systèmes, France) and followed the ASTM D638 Type IV standard as shown in Fig 1. The printer used for fabrication is the Artillery Sidewinder X2 3D printer. This printer has a large build volume of 300 x 300 x 400 mm. PETG carbon fibre filament was purchased and produced by SUNLU (SUNLU, Zhuhai, China). The specimens were printed with a 1.75 mm diameter of PETG with 20% carbon fibre reinforcement. Mechanical properties of the filament are presented in Table 1. The slicing software used to slice the CAD file to 3D printer G-code was Ultimaker Cura 5.3 software from Ultimaker.

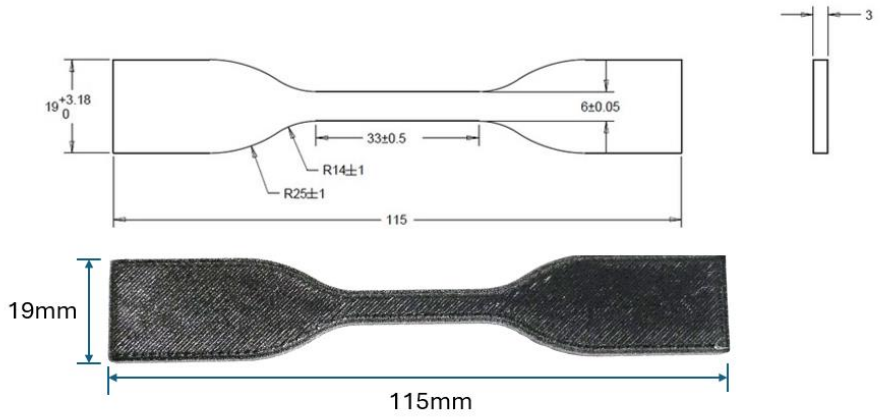

Fig. 1. Printed samples with its dimensions according to ASTM D638

Table 1. Mechanical properties of PETG carbon fibre filament.

Properties	Value
Density (g/cm^3)	1.34
Glass Transition Temperature (°C)	80
Tensile Strength (MPa)	56
Tensile Modulus (MPa)	5230
Tensile Elongation (%)	3
Flexural Strength (MPa)	80
Flexural Modulus (MPa)	5740

2.2 Materials and Method

According to Taguchi L9 module, 9 run of experiment have been conducted with each run repeated three time to ensure consistency and robustness of data. A total of 27 specimens were printed according to the Taguchi L9 module with different combinations of layer thickness, infill density, and printing speed, and all other printing parameter are kept constant as shown in Table 3 and Table 4. The tensile tests were performed using the SHIMADZU Autograph AGSX Universal Tensile machine with a 10 mm/min speed.

Table 2. Printing parameters

Process parameter	Value
Layer Thickness (mm)	0.2, 0.3, 0.4
Infill Density (%)	20, 50, 80
Printing speed (m/s)	30, 60, 90
Infill pattern	Rectilinear
Extruder temperature (C˚)	230
Build plate temperature (C˚)	80
Extrusion flow rate %	100

Table 3. Taguchi L9 experimental module

Run	Layer Thickness (mm)	Infill Density (%)	Printing Speed (mm/s)
1	0.2	20	30
2	0.2	50	60
3	0.2	80	90
4	0.3	20	60
5	0.3	50	90
6	0.3	80	30
7	0.4	20	90
8	0.4	50	30
9	0.4	80	60

3. RESULTS AND DISCUSSION

Each of the 27 samples was created using the Artillery Sidewinder X2, and subsequently subjected to a tensile test. Fig 2 illustrates 27 printed samples. Fig 3 shows samples from each run of experiment before and after tensile testing. The results obtained are displayed in Table 2 below.

Fig. 2. 27 printed samples

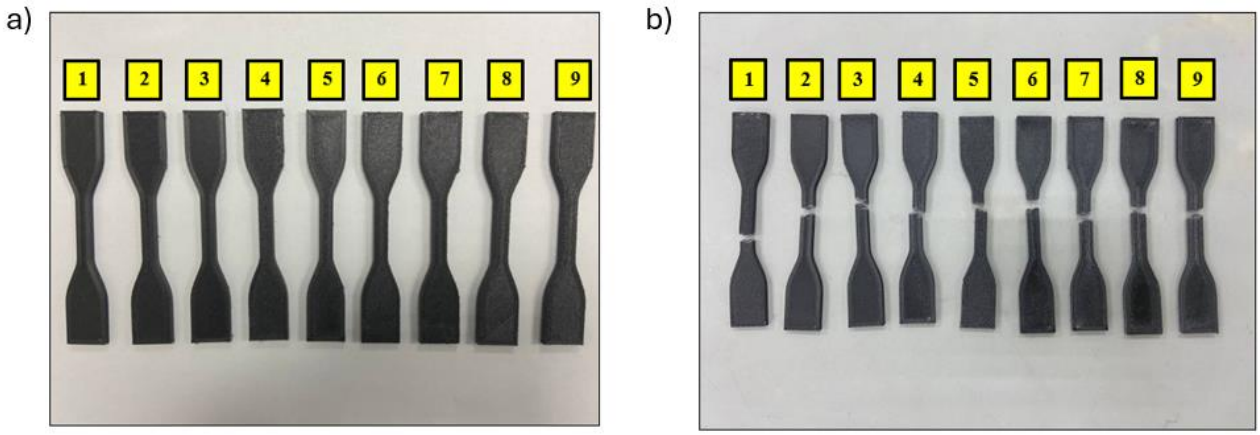

Fig. 3. Samples from each run before and after tensile testing

Table 3. Results from the tensile test

Run	Layer Thickness (mm)	Infill Density (%)	Printing Speed (mm/s)	Maximum stress (MPa)
1	0.2	20	30	52.6750
2	0.2	50	60	54.0529
3	0.2	80	90	66.8517
4	0.3	20	60	52.0487
5	0.3	50	90	56.2639
6	0.3	80	30	66.1558
7	0.4	20	90	53.3606
8	0.4	50	30	59.7259
9	0.4	80	60	62.9534

From table 3, it can be observed that the highest maximum stress is achieved in Run 3, with a value of 66.8517 MPa, highlighting the significant influence of high infill density (80%) and fine layer thickness (0.2 mm) on tensile strength. Meanwhile, the lowest maximum stress is observed in Run 4, with a value of 52.0487 MPa, demonstrating the impact of lower infill density (20%) and a moderate layer thickness (0.3 mm). Figure 4 show the breaking stress-strain curve for Run 3, Run 6 and Run 8 to provide a detailed representation of the mechanical response of the sample under tensile loading. These run were chosen because of their mechanical properties and variation in printing parameters, that can provide comprehensive view of the material behvaiour.

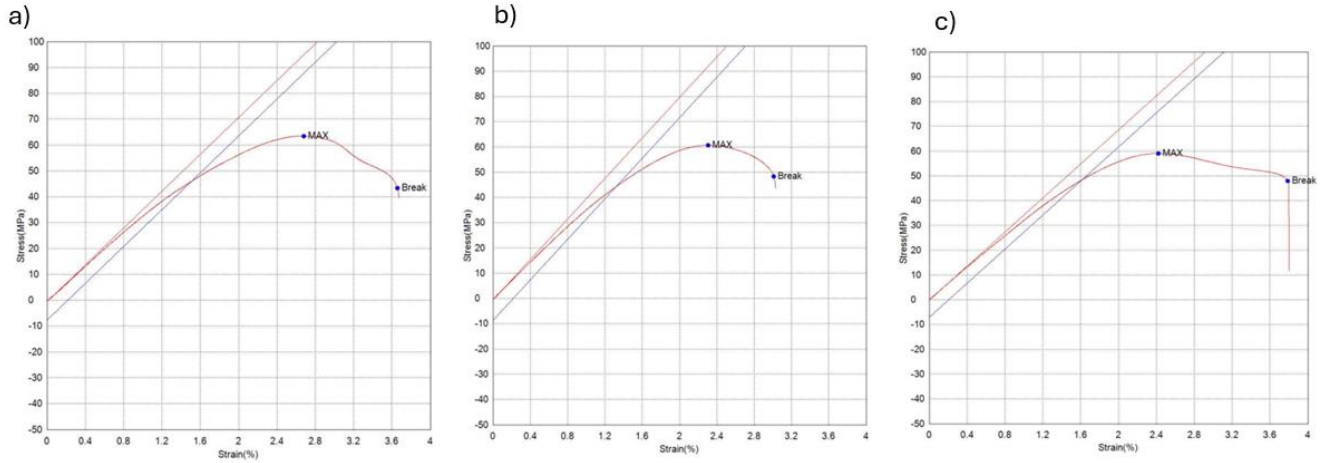

Fig. 4. Breaking curve of stress – strain curve from a) Run 3, b) Run 6 and c) Run 8

Fig 4 a), shows the breaking stress-strain curve for Run 3 (Layer Thickness: 0.2 mm, Infill Density: 80%, Printing Speed: 90 mm/s). The samples from this runs shown the highest tensile strength observed in the study, reaching a maximum stress of 66.8517 MPa and breaking stress of 43 MPa. The high infill density and fine layer thickness contribute to strong interlayer bonding, resulting in superior mechanical properties. The two parallel lines, colored red and blue, represent the elastic modulus boundaries. The red line usually represents the upper boundary of the elastic modulus, signifying the maximum stiffness observed before the material starts to yield, while the blue line represents the lower boundary, capturing the onset of deviation from ideal elastic behavior. The close and parallel nature of these lines indicates a consistent and high elastic modulus, suggesting reliable stiffness and minimal variability in the material's elastic response under these printing conditions. Fig 4 b) illustrates the breaking stress-strain curve for Run 6 (Layer Thickness: 0.3 mm, Infill Density: 80%, Printing Speed: 30 mm/s). The sample from this run exhibits a high maximum stress and the highest breaking stress among the 0.3 mm layer thickness samples, demonstrating the benefits of high infill density and moderate layer thickness. Run 6 achieves a maximum stress of 66.1558 MPa and a breaking stress of 48 MPa. The lower printing speed enhances layer adhesion, contributing to the material's high strength and durability. The parallel lines in this graph highlight the elastic modulus boundaries, with the red line representing the upper boundary and the blue line the lower boundary. The consistent spacing between these lines signifies a uniform elastic response, confirming the material's predictable and robust mechanical properties. Fig 4 c) provides the breaking stress-strain curve for Run 8 (Layer Thickness: 0.4 mm, Infill Density: 50%, Printing Speed: 30 mm/s). This run offers a balanced perspective on the effects of thicker layers and moderate infill density, with maximum stress of 59.7259 MPa and a breaking stress of 49 MPa. This configuration highlights the trade-offs between layer thickness and infill density, demonstrating that even with a thicker layer, high mechanical performance can be achieved through optimal infill and printing speed. The parallel lines in this curve represent the elastic modulus boundaries, showing a consistent elastic response with minimal variability, indicated by the close and parallel positioning of the red and blue lines.

3.1 Effect of Infill Density on Tensile Strength

The result from Table 3 reveals that increasing the infill density generally leads to higher tensile strength. As shown in Fig. 5, at an infill density of 80%, the sample attains high solidity, resulting in a densely packed structure with a higher concentration of carbon fibre reinforcement with a minimal gap between adjacent lines. Thus, the part exhibits increased density and greater resistance to applied load, resulting in the highest achievable strength at this infill rate.

Meanwhile, it can be seen from Fig. 6 that at an infill density of 20%, there is an increased presence of void spaces or gaps within the printed part compared to sample 3. These voids occur between the printed layers and within the infill structure. These voids can act as stress concentrators and potential sites for failure under applied loads. Moreover, the interlayer adhesion may be compromised with less material filling the void spaces. This can result in weaker bonding between layers, reducing the overall structural integrity of the printed part.

The relationship between infill density and tensile strength was consistent with prior research findings. Elongation at break decreases as infill density increases the solidification rate [15]. This behaviour is also influenced by the stronger bonding between the succeeding layers that result from reduced air gaps [5]. Therefore, by increasing the infill density, it effectively increases the amount of carbon fibre reinforcement within the printed object, resulting in improved load-bearing capacity and resistance to tensile forces.

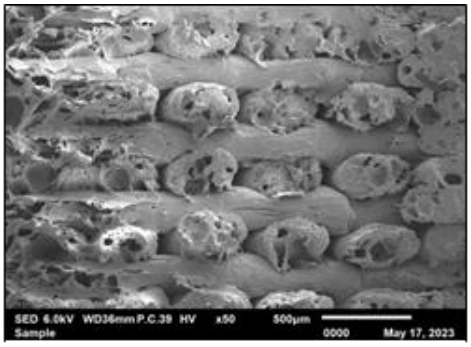

Fig. 5. Microstructure of sample with 80% infill density

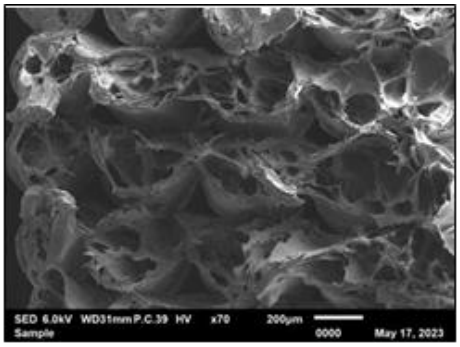

Fig. 6. Microstructure of sample with 20% infill density

3.2 Impact of Layer Thickness on Tensile Strength

The tensile strength value fluctuates depending on the layer thickness level. Nevertheless, no significant differences was observed across the various degrees of layer thickness for sample with same infill density. For instance, at 20% infill density, the tensile strength was 52.675, 52.0487, and 53.3606 MPa for layer thicknesses of 0.2, 0.3, and 0.4 mm, respectively. PETG carbon fibre filaments generally have higher structural integrity and improved interlayer adhesion than standard PETG filaments due to addition of carbon fibres which functions as a bonding agent between the layers. The enhanced interlayer adhesion can allow for greater flexibility in choosing the layer thickness without significantly compromising the printed parts' mechanical properties. This is supported by prior research, which revealed that the thickness of the layers had a detrimental impact on the tensile strength of the printed samples [16-17].

3.3 Impact of Printing Speed on Tensile Strength

Based on the data in Table 2, the printing speed does not consistently affect tensile strength. The different combination of parameter settings for sample 3 with the combination of 0.2 mm layer thickness, infill density 80%, and printing speed 90 mm/s has the highest average tensile strength value, which is 66.8517 MPa, followed by samples 6 and 9, which have the average tensile strength value of 66.1558 and 62.9534 MPa, respectively. Sample 6 has a printing speed of 30 mm/s, while sample 9 has 90 mm/s. Supporting this observation, a study has used an analysis of variance to assess the impact of various printing parameters on the tensile strength and surface roughness of nanographite-reinforced PLA filaments. Their findings indicate that printing speed does not significantly affect tensile strength, which aligns with the data presented in Table 3. This suggests that the influence of printing speed on tensile strength may be more dependent on the specific material and settings used rather than a universal parameter that consistently affects performance across different materials and print conditions [18].

3.4 Analysis of Variance (ANOVA)

The Analysis of Variance (ANOVA) was used to enable the comparison of means across two or more groups. This statistical test is considered parametric in nature, as it operates under the assumption that the underlying data follows a normal distribution. The result obtained from ANOVA is shown in Table 4.

Table 4. Results from ANOVA

Source	DF	Adj SS	Adj MS	F-Value	P-Value
Regression	3	240.836	80.279	11.48	0.011
Layer Thickness	1	1.0009	1.009	0.14	0.720
Infill Density	1	293.106	239.106	34.20	0.002
Printing Speed	1	0.721	0.721	0.10	0.761
Error	5	34.955	6.991		
Total	8	275.791			

A p-value of 0.05 is used as the significance level for the ANOVA. According to the results presented in Table 3, the infill density (p = 0.002) has a statistically significant impact on the response variable, as its p-value is

lower than 0.05. The observed disparities in tensile strength among various infill density levels are improbable to be random and can be ascribed to the variations in infill density. Meanwhile, based on the ANOVA, the layer thickness (p = 0.720) and printing speed (p = 0.761) show no significant impact on the tensile strength. The data illustrated in Fig. 6 shows that increasing the infill density from 20% to 80% results in a corresponding improvement in the tensile strength of the specimen. While the other two parameters may not have a significant impact on the results, it is still important to consider them to improve the tensile strength of the specimen.
In Fig. 7, the interaction of layer thickness and infill density provides evidence that the higher infill density gives better tensile strength. The intersection of lines between the three parameters suggests that the effect of one independent variable on the dependent variable differs depending on the level or values of the other independent variable.

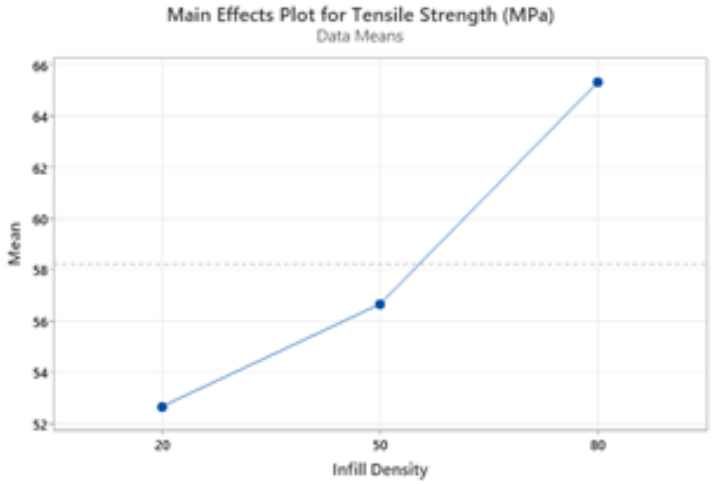

Fig. 7. Main effects plot for infill density

3.5 S/N Ratio and Means

The response table of the signal-to-noise ratio, which serves as a reference for selecting the optimal parameter level for each factor, is shown in Table 5. Delta and rank values have been employed to identify the parameter that holds significant influence over tensile strength. The first rank exhibited the greatest delta value, and vice versa. The analysis will clarify the primary parameter accountable for generating higher tensile strength.

Table 5. Response table for S/N ratios

Level	Layer Thickness (mm)	Infill Density (%)	Printing Speed (mm/s)
1	**35.20**	**34.43**	**35.46**
2	**35.25**	**35.06**	**34.99**
3	**35.35**	**36.30**	**35.35**
Delta	**0.15**	**1.86**	**0.47**
Rank	**3**	**1**	**2**

From the response table for means in Table 6, the infill density is ranked 1 (Delta = 12.63). The second rank is printing speed, followed by layer thickness. The selected rank is based on the largest to the lowest delta value. The main effects plot for the mean, as depicted in Fig. 8, clearly demonstrates the impact of process parameters. This plot aims to distinguish the various parameters that impact the response of tensile strength, as evidenced by each parameter level. In the context of main effect plots, a point near the average horizontal line indicates a relatively lower level of significance for the effect being analyzed. Therefore, the point exhibiting the highest degree of inclination holds the greatest impact on the response, as the mean line is inclined with respect to the x-axis. According to the results shown in Fig. 5, the infill density significantly impacts the tensile strength.
The larger-is-better type objective function was utilized to govern the response during the calculation of tensile strength. Process parameter levels were identified to optimize tensile strength. An increased signal-to-noise ratio proved to be linked to improved mechanical characteristics. Fig. 9 illustrates that an augmentation in the signal-to-noise ratio is directly associated with an elevation in the tensile strength. Table 6 presents the precise values

and levels of the optimal process parameters that were extrapolated from the linear graphs. To get the highest tensile strength, it is recommended to use the following process parameters: a layer thickness of 0.4 mm, an infill density of 80%, and a print speed of 30 mm/s.

Table 6. Response table for means

Level	Layer Thickness (mm)	Infill Density (%)	Printing Speed (mm/s)
1	57.86	52.69	59.52
2	58.16	56.68	56.35
3	58.68	65.32	58.83
Delta	0.82	12.63	3.17
Rank	3	1	2

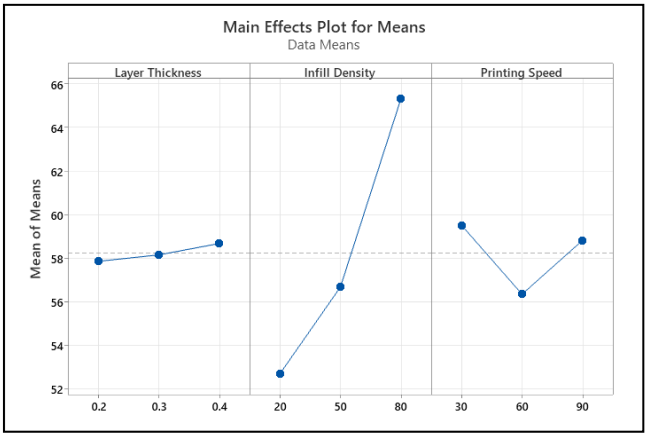

Fig 8. Main effects plot for means

Table 7. Optimum parameter settings

Layer thickness (mm)	Infill density (%)	Printing speed (mm/s)
0.4	80	30

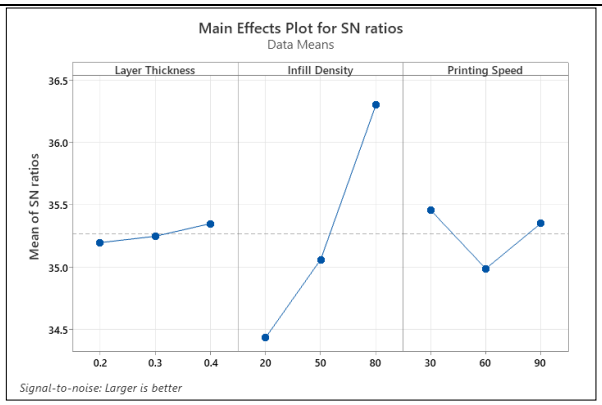

Fig. 9. Main effects plot for means

Consequently, increasing the value for layer thickness, infill density, and lower printing speed results in improved tensile strength. Higher infill densities generally increase tensile strength by providing a denser internal structure with more reinforcement. On the other hand, while higher printing speeds may improve productivity, they can negatively impact tensile strength. Finding a balance between speed and quality is crucial to prevent detrimental effects on the material properties. Slower printing speeds often result in better tensile strength, allowing for proper material deposition, bonding, and fiber alignment. By systematically varying these parameters and analyzing the resulting tensile strength, it is feasible to determine the most effective configuration of layer thickness, infill density, and printing speed for PETG carbon fibre 3D printing. This

optimization method can lead to the production of high-quality, durable parts with superior tensile strength, meeting the specific requirements of the intended applications.

4. CONCLUSION

This research aimed to improve the FDM 3D printing parameters for the tensile strength of PETG carbon fibre by employing the Taguchi approach. The investigation concentrated on three parameters: the thickness of the layers, the density of the infill, and the speed of the printing process. The findings indicated that the tensile strength of PETG carbon fibre was considerably influenced by infill density, whereas layer thickness and printing speed had less impact. The most effective configuration of parameters was determined to be a layer thickness of 0.4 mm, 80% infill density, and 30 mm/s printing speed. This research contributes to the knowledge of 3D printing with PETG carbon fibre, a composite material with potential applications in various fields requiring high strength and rigidity. The findings can help 3D printing users and manufacturers improve the quality and performance of their products by selecting the appropriate printing parameters. The research also demonstrates the usefulness of the Taguchi technique as a statistical method for optimizing 3D printing processes.

This research has some limitations that suggest directions for future work. First, the sample size was relatively small, and only one type of PETG carbon fibre filament was used. Therefore, more experiments with larger samples and different brands of filaments are needed to validate and generalize the results. Second, only tensile strength was measured as the response variable. Other mechanical properties, such as modulus, elongation, and impact strength, should also be investigated to obtain a more comprehensive understanding of the behavior of PETG carbon fibre under different loading conditions. Third, this research did not consider other factors that may affect the 3D printing quality, such as nozzle diameter, extrusion temperature, cooling fan speed and environmental humidity. These factors should be included in future studies to optimize the 3D printing parameters for PETG carbon fibre more effectively.

Funding: This paper has received no external funding.
Conflicts of Interest: There is no conflict of interest.

REFERENCES

1. Ngo, T., Kashani, A., Imbalzano, G., Nguyen, K., Hui, D. (2018). *Additive manufacturing (3D printing): A review of materials, methods, applications and challenges*. Composites. Part B, Engineering, 143, 172–196. https://doi.org/10.1016/j.compositesb.2018.02.012

2. Chohan, J. S., Kumar, R., Yadav, A., Chauhan, P., Singh, S., Sharma, S., Li, C., Dwivedi, S. P., Rajkumar, S. (2022). *Optimization of FDM printing process parameters on surface finish, thickness, and outer dimension with ABS polymer specimens using Taguchi orthogonal array and genetic algorithms*. Mathematical Problems in Engineering, 1–13. https://doi.org/10.1155/2022/2698845

3. Valvez, S., Silva, A. P., & Reis, P. N. B. (2022). *Compressive Behaviour of 3D-Printed PETG Composites*. Aerospace, 9(3), 1–13. https://doi.org/10.3390/aerospace9030124

4. García, E., Núñez, P. J., Caminero, M. A., Chacón, J. M., Kamarthi, S. (2022). *Effects of carbon fibre reinforcement on the geometric properties of PETG-based filament using FFF additive manufacturing*. Composites Part B: Engineering, 235, 109766. https://doi.org/10.1016/j.compositesb.2022.109766

5. Kichloo, A. F., Raina, A., Haq, M. I. U., Wani, M. S. (2022). *Impact of Carbon Fiber Reinforcement on Mechanical and Tribological Behavior of 3D-Printed Polyethylene Terephthalate Glycol Polymer Composites—An Experimental Investigation*. Journal of Materials Engineering and Performance, 31(2), 1021–1038. https://doi.org/10.1007/s11665-021-06262-6

6. Nabipour, M., Akhoundi, B. (2021). *An experimental study of FDM parameters effects on tensile strength, density, and production time of ABS/Cu composites*. Journal of Elastomers and Plastics, 53(2), 146–164. https://doi.org/10.1177/0095244320916838

7. Mishra, A., Srivastava, V., Gupta, N. K. (2021b). *Additive manufacturing for fused deposition modeling of carbon fiber–polylactic acid composites: the effects of process parameters on tensile and flexural properties*. Functional Composites and Structures, 3(4), 045007. http://dx.doi.org/10.1088/2631-6331/ac3732

8. Kamaal, M., Anas, M., Rastogi, H., Bhardwaj, N., Rahaman, A. (2020). *Effect of FDM process parameters on mechanical properties of 3D-printed carbon fibre–PLA composite.* Progress in Additive Manufacturing, 6, 63-69. https://doi.org/10.1007/s40964-020-00145-3

9. Kumar, M., Khan, M., Mishra, S. (2020). *Effect of fused deposition machine parameters on tensile strength of*

printed carbon fiber reinforced PLA thermoplastics. Materials Today: Proceedings, 27, 1505-1510. https://doi.org/10.1016/j.matpr.2020.03.033
10. Ranjan, R, Raote, P, Bajpai, V. (2020), *Woven Carbon Fiber Reinforced Laminate Matrix Composite Through Fused Deposition Modeling*. Proceedings of the ASME 2020 15th International Manufacturing Science and Engineering Conference. Volume 1: Additive Manufacturing; Advanced Materials Manufacturing; Biomanufacturing; Life Cycle Engineering; Manufacturing Equipment and Automation. Virtual, Online. September 3, 2020. V001T01A007. ASME. https://doi.org/10.1115/MSEC2020-8282
11. Heidari-Rarani, M., Ezati, N., Sadeghi, P., Badrossamay, M. (2020). *Optimization of FDM process parameters for tensile properties of polylactic acid specimens using Taguchi design of experiment method*. Journal of Thermoplastic Composite Materials, 35, 2435 - 2452. https://doi.org/10.1177/0892705720964560
12. Mishra, A., Srivastava, V., Gupta, N. K. (2021). *Additive manufacturing for fused deposition modeling of carbon fiber–polylactic acid composites: the effects of process parameters on tensile and flexural properties*. Functional Composites and Structures, 3(4), 045007. http://dx.doi.org/10.1088/2631-6331/ac3732
13. Huynh, L., Nguyen, H., Nguyen, H., Phan, L., Tran, T. (2019). *Effect of Process Parameters on Mechanical Strength of Fabricated Parts using the Fused Deposition Modelling Method*. Journal of the Korean Society for Precision Engineering, 36(8), 705–712. https://doi.org/10.7736/KSPE.2019.36.8.705
14. Valvez, S., Silva, A. P., & Reis, P. (2022). *Optimization of printing parameters to maximize the mechanical properties of 3D-Printed PETG-Based parts*. Polymers, 14(13), 2564.
15. Le, D., Nguyen, C.H., Pham, T.H.N. et al. *Optimizing 3D Printing Process Parameters for the Tensile Strength of Thermoplastic Polyurethane Plastic.* J. of Materi Eng and Perform, 32, 10805–10816 (2023). https://doi.org/10.1007/s11665-023-07892-8
16. Alarifi, I. M. (2023). *PETG/carbon fiber composites with different structures produced by 3D printing*. Polymer Testing, 120, 107949. https://doi.org/10.1016/j.polymertesting.2023.107949
17. Bhandari, S., Lopez-Anido, R. A., Gardner, D. J. (2019). *Enhancing the interlayer tensile strength of 3D printed short carbon fiber reinforced PETG and PLA composites via annealing*. Additive Manufacturing, 30, 100922. https://doi.org/10.1016/j.addma.2019.100922
18. Fadillah, F., Suryanto, H., Suprayitno, S. (2023). *Study on Effect of 3D Printing Parameters on Surface Roughness and Tensile Strength Using Analysis of Variance*. Journal of Mechanical Engineering Science and Technology (JMEST), *7*(2), 96, https://doi.org/10.17977/um016v7i22023p096

Received: February 22th, 2024 / Accepted: December 15th, 2024 / Paper available online: December 20th, 2024